One-dimensional alkali-doped C_{60} chains encapsulated in BN nanotubes

Takashi Koretsune, Susumu Saito, and Marvin L. Cohen

Phys. Rev. B **83**, 193406 — Published 20 May 2011

DOI: 10.1103/PhysRevB.83.193406

One-dimensional alkali-doped C_{60} chain encapsulated in BN nanotubes

Takashi Koretsune, Susumu Saito
Department of Physics, Tokyo Institute of Technology,
2-12-1 Oh-okayama, Meguro-ku, Tokyo 152-8551, Japan

Marvin L. Cohen
Department of Physics, University of California, Berkeley, California 94720
Materials Sciences Division, Lawrence Berkeley
National Laboratory, Berkeley, California 94720

Abstract

We study the energetics, the electronic structures and the electron-phonon couplings of a one-dimensional potassium-doped C_{60} chain encapsulated in a boron nitride nanotube using the framework of the density-functional theory. We demonstrate that the reaction of potassium doping is exothermic and the resulting material is one-dimensional metal where conducting electrons are only in the C_{60} chain. Interestingly, the Fermi-level density of states has a peculiar pressure dependence and can be larger than those in the three-dimensional alkali-doped fullerene compounds, indicating the possibility of various phase transitions. We also discuss the electron-phonon couplings and the possibility of superconductivity.

PACS numbers: 73.22.-f,71.15.Mb,74.70.Wz

Since the discovery of carbon nanotubes[1], these unique one-dimensional materials have attracted considerable attention. The so-called carbon peapod, that is, a chain of C_{60} encapsulated in the carbon nanotubes[2], is one of the remarkable applications of the nanoscale tubular structure. As in the case of the carbon nanotubes, boron nitride nanotubes (BNNTs)[3–5] are rolled-up monolayer hexagonal boron nitride sheets and have similar geometrical and mechanical properties. However, contrary to the carbon nanotubes that can be metallic or semiconducting depending on the diameter and chirality[6], BNNTs have an energy gap of roughly 5 eV independent of the structure. Thus, BNNTs are stable electronically as well as geometrically, and are promising candidates for nanoscale design of novel materials that may be realized by confining atoms or molecules.

BNNTs can also host a one-dimensional C_{60} chain and form a BN peapod similar to the carbon peapod, which was first theoretically proposed[7] and experimentally synthesized soon after[8]. Interestingly, there are some differences between the carbon peapod and the BN peapod [7–9]. Particularly, in the BN peapod, the conduction band bottom is inside the original gap of BNNTs and is composed of t_{1u} states on the C_{60} whereas the conduction bands of C_{60} in the carbon peapod are mixed with those of the carbon nanotube[10] except for the case of semiconducting carbon nanotubes with a large band gap[11]. Therefore, carrier doping in the BN peapod is an interesting approach to achieve a novel one-dimensional metal and superconductor made of C_{60} as in the case of three-dimensional alkali-doped C_{60} compounds[12]. In fact, Timoshevskii *et al.*[13] theoretically predicted the possibility of carrier doping using potassium atoms outside the BNNTs. However, in this case, since there is a large distance between C_{60} and potassium atom, potassium 4s states are pushed down and start to mix with t_{1u} originated states of the C_{60} with increasing doping level even for the (9,9) BNNT that has slightly small diameter for C_{60} encapsulation[7]. This indicates that carriers are not efficiently doped in this geometry and that the materials might have a high reactivity.

To discuss the possibility of carrier doping in the BN peapod further, we put potassium atoms inside the BNNTs and construct a potassium doped C_{60} chain encapsulated in the BNNTs (K_xC_{60}@BNNTs). Using first-principle calculations, we show that the potassium doping inside the BNNTs is energetically favorable and that the doped carriers are almost on the C_{60}, which is in sharp contrast to the case of potassium doping into carbon peapod where doped carriers are both on the C_{60} and nanotube[14]. In addition, it is found that the

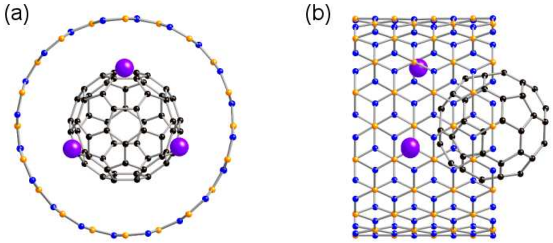

FIG. 1: (Color online) Geometry of K_3C_{60}@BN(10,10): (a) top view and (b) side view. Tube radius for nitrogen atoms (blue circle) is approximately 0.03 Å longer than that for boron atoms (yellow circle).

density of states at the Fermi level varies depending on the doping level and can be large in some cases. Thus, we also discuss the effect of pressure, which plays a crucial role in three-dimensional alkali-doped C_{60} compounds, and the electron-phonon couplings to examine the possibility of superconductivity.

Our calculations have been performed within the local-density approximation (LDA)[15, 16] based on the density-functional theory (DFT). We use ultrasoft pseudopotentials to describe the electron-ion interaction[17]. The valence wave functions and charge densities are expanded in a plane-wave basis set with cutoff energies of 30 Ry and 200 Ry, respectively. We adopt a supercell approach[18] in the directions perpendicular to the tube axis and keep the long interwall distance of at least 10 Å. Atomic positions are relaxed until all force components in the system are less than 3 meV/Å. Integration over a one-dimensional Brillouin zone is carried out using the four k-points. To calculate phonon spectra and electron-phonon interactions, we utilize density functional perturbation theory[19–21].

To construct a peapod, we use a (10,10) BN nanotube. Its optimized length of the unit cell along the tube axis is 2.49 Å, which is close to one fourth of a lattice constant of the optimized weakly interacting C_{60} chain, 9.86 Å, where pentagons are facing each other. Therefore, we put each C_{60} inside the (10,10) BN nanotube with four unit cells of BN nanotube and impose the commensurability condition. The interwall distance between the (10,10) BN nanotube and the C_{60} is found to be about 3.1 Å, which is close to the interlayer distances of graphite (3.34 Å), h-BN (3.33 Å), and the superlattice of graphene an BN monolayer (3.24 Å)[22]. Potassium atoms are located between C_{60}s inside the nanotube.

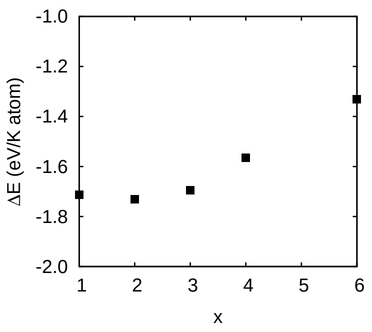

FIG. 2: Reaction energies, ΔE, of K_xC_{60}@BN(10,10).

For example, the optimized geometry of K_3C_{60} encapsulated in the (10,10) BN nanotubes (K_3C_{60}@BN(10,10)) is shown in Fig. 1.

To confirm the energetic stability of K_xC_{60}@BN(10,10), we calculated the energy difference, ΔE, on the reaction between bulk potassium and the BN-peapod given by xK + C_{60}@BN(10,10) $\rightarrow$ K_xC_{60}@BN(10,10) - $x\Delta E$. As shown in Fig. 2, the reaction is exothermic with the energy of approximately 1.7 eV per K atom for $x \leq 3$, which is larger than the energy of 0.56 eV per K atom for the external deposition[13]. Note that reaction energies are smaller for $x \geq 4$. This indicates that the potassium-atom disproportionation, which may occur for $x < 3$ because of the approximately same exothermic energies for $x \leq 3$, is avoidable for $x \geq 3$.

The electronic band structures of (10,10) BN nanotube and K_xC_{60}@BN(10,10) with $x = 0, 1, 2,$ and 3 are presented in Figs. 3 (a)-(e). As discussed in the previous theoretical study for C_{60}@BN(10,10)[7], there are states inside the gap of the BNNTs. For example, all states between 1 eV and 4 eV in Fig. 3 (b) are from C_{60}. To examine the origin of the states around the Fermi level, we compare the band structure of K_xC_{60}@BN(10,10) with that of one-dimensional K_xC_{60} in Figs. 3 (f)-(i), where the geometries of K_xC_{60} are the same in the K_xC_{60}@BN(10,10). Apparently, the band structures of K_xC_{60} and K_xC_{60}@BN(10,10) show good agreement, suggesting that the effect of the BNNTs is negligible as far as the band structures around the Fermi level are concerned. Note that this also indicates that the most of the following discussion should be applicable to K_xC_{60}@BNNT systems with different chirality nanotubes as far as the diameter is similar to (10,10) BN nanotube.

Comparing the band structures for $x = 0$ - 3 in Figs. 3 (f)-(i), the qualitative features of band dispersions do not change much with potassium doping whereas the Fermi level shifts

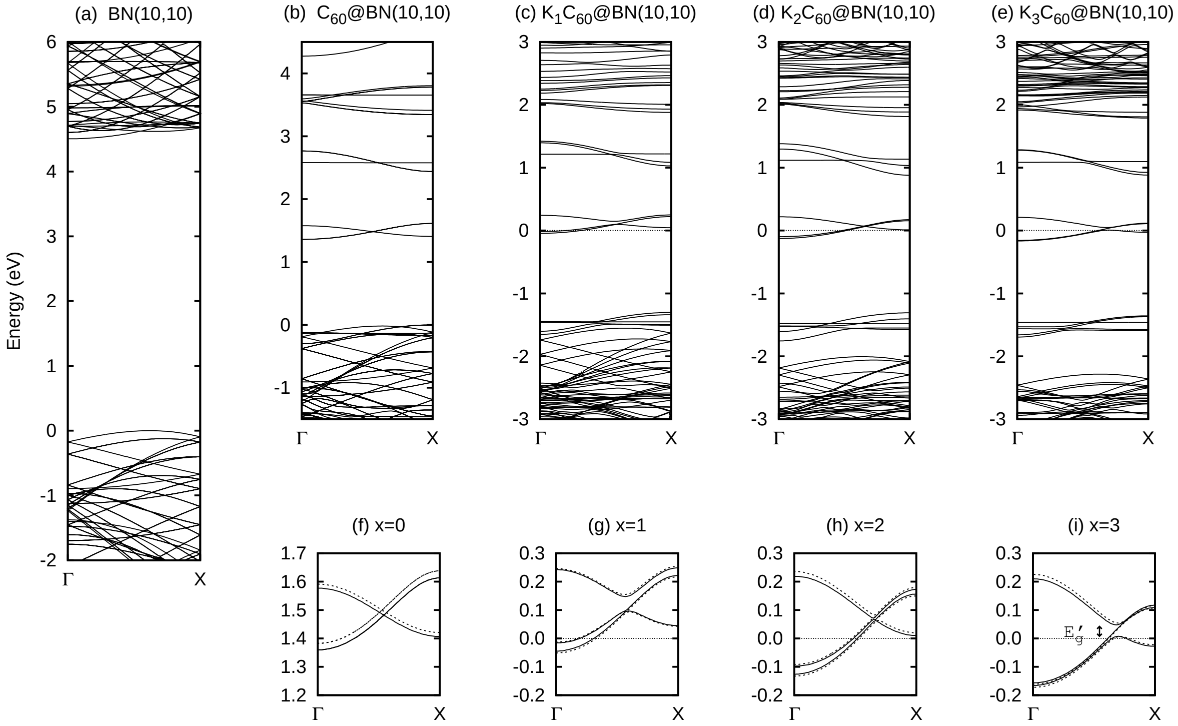

FIG. 3: Electronic band structures of (a) BN(10,10) and K_xC_{60}@BN(10,10) with (b) $x = 0$, (c) $x = 1$, (d) $x = 2$ and (e) $x = 3$. Details of the band structures around the Fermi level are shown for (f) $x = 0$, (g) $x = 1$, (h) $x = 2$, and (i) $x = 3$ (solid lines), where, for comparison, we also plot the band structures of K_xC_{60} that has same geometry with K_xC_{60}@BN(10,10) (dashed curve). Valence band top or Fermi level (dotted line) are set to be zero.

upwards with increasing the number of potassium atoms. This suggests that the potassium doping can be understood as a carrier doping into the C_{60} t_{1u} states at the bottom of the conduction band in one-dimensional C_{60} chain as in the case of fcc K_3C_{60}. Contrary to the three-dimensional case, the symmetry of the one-dimensional K_xC_{60} is low. Therefore, the energy levels of three states, which are almost degenerate at $x = 0$, shift independently with potassium doping and as a result, the bandwidth increases. Furthermore, there is a gap, E'_g, between two states for $x = 1$ and $x = 3$ as shown in Fig. 3 (i). The Fermi level densities of states are 10.1, 4.9, and 12.4 states/eV/spin/C_{60} for $x = 1, 2,$ and 3, respectively, which are comparable to the values of the fcc K_3C_{60}[23, 24].

In the three-dimensional alkali-doped C_{60} systems, the distance between C_{60}s plays a crucial role. Thus, it is important to study the pressure dependence of the electronic structures.

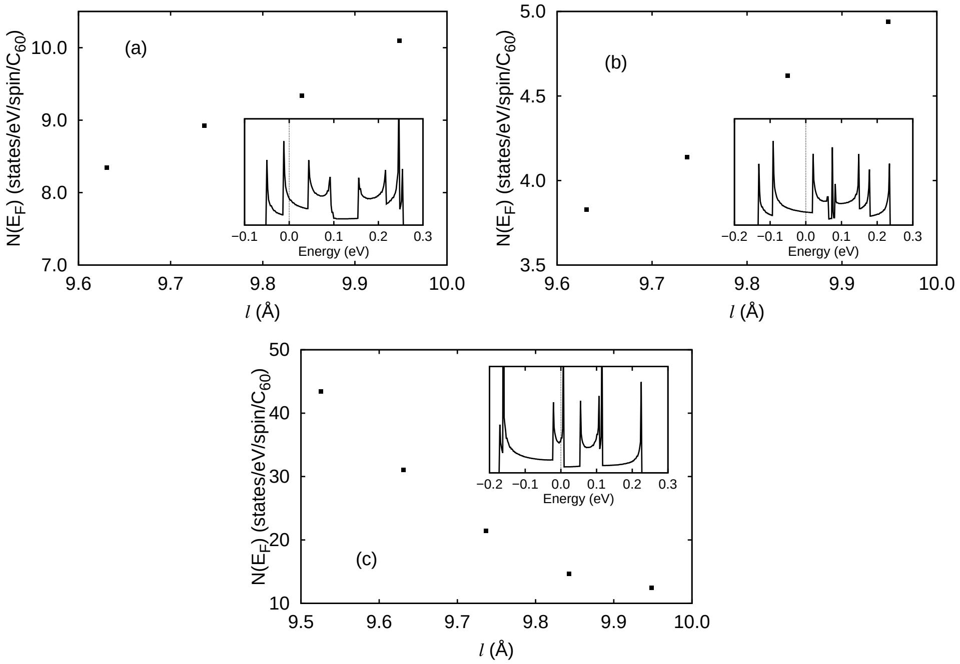

FIG. 4: Densities of states at the Fermi level, $N(E_F)$, as a function of lattice constant, l, for K_xC_{60} with (a) $x = 1$, (b) $x = 2$, and (c) $x = 3$. Densities of states, $N(E)$, around the Fermi level at $l = 9.86$ Å are shown in the inset.

Naively, it is almost impossible to calculate the pressure dependence because we can only compute a commensurate structure whereas the pressure changes the length of the BNNT and the distance between C_{60}s differently. In this case, however, BNNTs only act as a cage to ensure the one-dimensional structure of K_xC_{60} and do not affect the electronic structures inside the original fundamental gap of BNNTs. Therefore, we vary the lattice constant of commensurate K_xC_{60}@BN(10,10) and optimize the geometry to obtain the approximate geometry of K_xC_{60} in the incommensurate K_xC_{60}@BN(10,10). Using this “optimized” K_xC_{60}, we compute the pressure dependence of the total energy and the electronic band structure.

Figure 4 plots the Fermi level density of states, $N(\epsilon_\mathrm{F})$, of the “optimized” K_xC_{60} as a function of lattice constant, l, as well as densities of states around the Fermi level, $N(E)$. In the case of $x = 1$ and 2, $N(\epsilon_\mathrm{F})$ grows with increasing the distance between C_{60}s because of a result of a bandwidth decrease as in the fcc alkali-doped C_{60} systems. On the contrary, in the case of $x = 3$, $N(\epsilon_\mathrm{F})$ grows with decreasing the distance between C_{60}s. This unexpected behavior of the $x = 3$ case can be understood as follows. Because of the one-dimensional geometry, there is a gap between two bands, E'_g, as shown in Fig. 3 (i), and E'_g increases with decreasing distance between C_{60}s. Thus, the van Hove singularity gets close to the Fermi level, which results in the increase of $N(\epsilon_{\mathrm{F}})$. Note that we can estimate the optimized lattice constant using the energy of "optimized" K_xC_{60}. For $x = 3$, the optimized lattice constant is 9.67 Å indicating $N(\epsilon_{\mathrm{F}}) \sim 27$ states/eV/spin/C_{60} at the ambient pressure.

To discuss the possibility of superconductivity, we compute the phonon frequencies and electron-phonon couplings using the "optimized" K_3C_{60} chain with a lattice constant of 9.67 Å. Here, we only consider the intramolecular modes, which are expected to be almost same with or without the BNNT and be important for superconductivity as in the fcc K_3C_{60} case. The electron-phonon coupling constant, λ, can be obtained from

$$\lambda = \frac{2}{N(\epsilon_{\mathrm{F}})} \sum_{\boldsymbol{q},\nu} \frac{1}{\omega_{\nu\boldsymbol{q}}} \sum_{n,m,\boldsymbol{k}} |g^{\nu}_{n\boldsymbol{k},m\boldsymbol{k}+\boldsymbol{q}}|^2 \delta(\epsilon_{n\boldsymbol{k}})\delta(\epsilon_{m\boldsymbol{k}+\boldsymbol{q}}), \tag{1}$$

where $\omega_{\nu\boldsymbol{q}}$ is the energy of the νth phonon with the wave vector $\boldsymbol{q}$ and $g^{\nu}_{n\boldsymbol{k},m\boldsymbol{k}+\boldsymbol{q}}$ is the matrix element between the two electron states $n\boldsymbol{k}$ and $m\boldsymbol{k}+\boldsymbol{q}$ with respect to the potential created by the excitation of $\nu\boldsymbol{q}$ phonon. In the present case, however, we only consider the intramolecular modes that have almost dispersionless bands. Hence, we can neglect the momentum dependences of $\omega_{\nu\boldsymbol{q}}$ and $g^{\nu}_{n\boldsymbol{k},m\boldsymbol{k}+\boldsymbol{q}}$, and write[24–27]

$$\lambda/N(\epsilon_{\mathrm{F}}) = \sum_{\nu} \frac{1}{3^2\omega_{\nu\boldsymbol{0}}} \sum_{m,n=1}^{3} |g^{\nu}_{m\boldsymbol{k},n\boldsymbol{k}}|^2. \tag{2}$$

Here, both m and n refer to the three t_{1u}-originated states. For $\boldsymbol{k} = \boldsymbol{0}$, we obtain $\lambda/N(\epsilon_{\mathrm{F}}) = 0.078$ eV. It has been confirmed that for different $\boldsymbol{k}$ values, $\lambda/N(\epsilon_{\mathrm{F}})$ changes less than 5 % being consistent with the above assumption of neglecting the momentum dependences. Note that this value agrees with the one obtained for isolated C_{60}^{-3} molecule[28–31] as expected. Though we should consider the three dimensionality such as bundle formation to stabilize superconductivity, large $N(\epsilon_{\mathrm{F}})$ expected for K-doped C_{60} peapods with BN nanotubes suggests the larger λ and the higher transition temperature compared even with the fcc alkali doped C_{60} compounds.

To summarize, we have studied the electronic structures of potassium doped C_{60} encapsulated in the BN nanotubes. Our results suggest that K_3C_{60}@BNNT has a large Fermi level density of states and shows peculiar pressure dependence due to the one-dimensional structure. We have also computed the electron-phonon coupling and revealed that there is a possibility of superconductivity with a transition temperature similar to or larger than fcc alkali-doped C_{60} compounds.

We would like to thank J. Noffsinger for useful discussions. Numerical calculations were performed on TSUBAME Grid Cluster at Global Scientific Information and Computing Center of the Tokyo Institute of Technology. This work was partially supported by National Science Foundation Grant No. DMR07-05941, by the Director, Office of Science, Office of Basic Energy Sciences, Materials Sciences and Engineering Division, U.S. Department of Energy under contract No. DE-AC02-05CH11231, by Grant-in-Aid for Scientific Research (contract numbers 22740252, 22013005, and 19054005) and Elements Science and Technology Project from MEXT Japan, by Ishikawa Carbon Foundation, and by the Global Center of Excellence Program by MEXT Japan through the "Nanoscience and Quantum Physics" Project of the Tokyo Institute of Technology.

[1] S. Iijima, Nature **354**, 56 (1991).

[2] B. Smith, M. Monthioux, and D. Luzzi, Nature **396**, 323 (1998).

[3] A. Rubio, J. L. Corkill, and M. L. Cohen, Phys. Rev. B **49**, 5081 (1994).

[4] N. G. Chopra, R. J. Luyken, K. Cherrey, V. H. Crespi, M. L. Cohen, S. G. Louie, and A. Zettl, Science **269**, 966 (1995).

[5] M. L. Cohen, and A. Zettl, Physics Today **63**, 34 (2010).

[6] N. Hamada, S. Sawada, and A. Oshiyama, Phys. Rev. Lett. **68**, 1579 (1992).

[7] S. Okada, S. Saito, and A. Oshiyama, Physical Review B **64**, 201303 (2001).

[8] W. Mickelson, S. Aloni, W. Han, J. Cumings, and A. Zettl, Science **300**, 467 (2003).

[9] A. Trave, F. J. Ribeiro, S. G. Louie, and M. L. Cohen, Phys. Rev. B **70**, 205418 (2004).

[10] S. Okada, S. Saito, and A. Oshiyama, Phys. Rev. Lett. **86**, 3835 (2001).

[11] T. Miyake and S. Saito, Solid State Comm. **125**, 201 (2003).

[12] A. F. Hebard, M. J. Rosseinsky, R. C. Haddon, D. W. Murphy, S. H. Glarum, T. T. M. Palstra, A. P. Ramirez, and A. R. Kortan, Nature **350**, 600 (1991).

[13] V. Timoshevskii and M. Côté, Phys. Rev. B **80**, 235418 (2009).

[14] S. Okada, Phys. Rev. B **72**, 153409 (2005).

[15] D. M. Ceperley and B. J. Alder, Phys. Rev. Lett. **45**, 566 (1980).

[16] J. P. Perdew and A. Zunger, Phys. Rev. B **23**, 5048 (1981).

[17] D. Vanderbilt, Phys. Rev. B **41**, 7892 (1990).

[18] M. L. Cohen, M. Schluter, J. R. Chelikowsky, and S. G. Louie, Phys. Rev. B **12**, 5575 (1975).

[19] S. Baroni, S. de Gironcoli, A. D. Corso, and P. Giannozzi, Rev. Mod. Phys. **73**, 515 (2001).

[20] S. Y. Savrasov and D. Y. Savrasov, Phys. Rev. B **54**, 16487 (1996).

[21] P. Giannozzi, S. Baroni, N. Bonini, M. Calandra, R. Car, C. Cavazzoni, D. Ceresoli, G. L. Chiarotti, M. Cococcioni, I. Dabo, et al., J. Phys. Condens. Matter **21**, 395502 (2009).

[22] Y. Sakai, T. Koretsune, and S. Saito, submitted.

[23] A. Oshiyama and S. Saito, Solid State Comm. **82**, 41 (1992).

[24] O. Gunnarsson, Rev. Mod. Phys. **69**, 575 (1997).

[25] M. Lannoo, G. A. Baraff, M. Schlüter, and D. Tomanek, Phys. Rev. B **44**, 12106 (1991).

[26] C. M. Varma, J. Zaanen, and K. Raghavachari, Science **254**, 989 (1991).

[27] M. Côté, J. C. Grossman, M. L. Cohen, and S. G. Louie, Phys. Rev. Lett. **81**, 697 (1998).

[28] M. Schluter, M. Lannoo, M. Needels, G. A. Baraff, and D. Tomanek, Phys. Rev. Lett. **68**, 526 (1992).

[29] V. P. Antropov, O. Gunnarsson, and A. I. Liechtenstein, Phys. Rev. B **48**, 7651 (1993).

[30] J. C. R. Faulhaber, D. Y. K. Ko, and P. R. Briddon, Phys. Rev. B **48**, 661 (1993).

[31] J. L. Janssen, M. Côté, S. G. Louie, and M. L. Cohen, Phys. Rev. B **81**, 073106 (2010).